

Emission of continuous coherent terahertz waves with tunable frequency by intrinsic Josephson junctions

Masashi Tachiki

National Institute for Materials Science, 1-2-1 Sengen, Tsukuba 305-0047, Japan

Mikio Iizuka, Kazuo Minami, Syogo Tejima, and Hisashi Nakamura

Research Organization for Information Science and Technology, 2-2-54 Nakameguro, Meguro-ku, Tokyo 153-0061, Japan

(Received 3 December 2004; revised manuscript received 7 February 2005; published 22 April 2005)

We present simulation results based on a model for emission of electromagnetic terahertz waves by high T_c superconductors. High T_c superconductors form naturally stacked Josephson junctions. When an external current and a magnetic field are applied to the sample, fluxon flow induces voltage. The voltage creates oscillating current through the Josephson effect and the current excites the Josephson plasma with terahertz frequency. The sample itself works as a cavity, and the input energy is stored in a form of standing wave of the Josephson plasma. A part of the energy is emitted as terahertz waves.

DOI: 10.1103/PhysRevB.71.134515

PACS number(s): 74.50.+r, 74.25.Gz, 85.25.Cp

We proposed a possibility of the emission of electromagnetic waves in high T_c superconductors.¹ Ustinov *et al.* have observed millimeter wave band radiation in flux flow states.² Hechtfisher *et al.* have observed centimeter wave emission from vortex flow in $\text{Bi}_2\text{Sr}_2\text{CaCu}_2\text{O}_{8+\delta}$.³ Barbara *et al.* have observed millimeter wave in Josephson-junction arrays.⁴ In the present paper we made simulation calculations to obtain continuous coherent terahertz waves, since the waves have various applications in scientific fields such as biology and information science. One of the hurdles for technological advancements in the terahertz region of electromagnetic waves is the development of sources for intense and continuous coherent terahertz waves. Therefore, we investigate a mechanism for emitting intense continuous and frequency tunable terahertz waves. In high temperature superconductors, the strongly superconducting CuO_2 layers and insulating layers are alternately stacked along the c axis of the crystals and form a naturally multiconnected Josephson junction called intrinsic Josephson junction (IJJ). In the IJJ there appears an excitation wave called Josephson plasma, the frequency of which is in the range of terahertz.^{5,6}

For investigating an emission mechanism of terahertz electromagnetic waves from the IJJ, we use the following model shown in Fig. 1. In this figure, the IJJ is shown in green and the electrodes of a normal metal (for example gold) are shown in yellow. An external magnetic field B applied in the direction of the y axis induces fluxons in this direction. The centers of the fluxons are in the insulating layers. In this system, the superconducting and normal currents almost uniformly flow in the direction indicated by J in Fig. 1. The fluxons flow in the negative direction of the x axis with a velocity v and induce a voltage difference in the direction of the z axis. This voltage creates an oscillating Josephson current along the z axis by the Josephson effect, when the temperature is sufficiently below T_c and the superconducting current is smaller than the maximum Josephson current. This oscillating current interacts strongly with the Josephson plasma due to the nonlinear nature of the system and intensively excites the Josephson plasma wave as shown

later. We use $\text{Bi}_2\text{Sr}_2\text{CaCu}_2\text{O}_{8+\delta}$ that is appropriate for the experiments, and apply a magnetic field and external currents near J_c the critical current to the IJJ. Subsequently, the frequencies of the plasma waves appear in the terahertz frequency range. The excited plasma wave is converted to an intense terahertz electromagnetic wave in the waveguide (dielectric) shown in orange in Fig. 1.

In accordance with the mechanism mentioned above, we now derive the equations for the simulation. The superconducting order parameter of the l th layer is expressed as $\psi_l(\mathbf{r}, t) = \Delta_l(\mathbf{r}, t)e^{i\varphi_l(\mathbf{r}, t)}$, where \mathbf{r} and t refer to the spatial and temporal coordinates, respectively. Since superconductivity in the CuO_2 layers is strong at low temperatures, we assume the amplitude $\Delta_l(\mathbf{r}, t)$ to be spatially and time independent. In this system, the current along the z axis perpendicular to the CuO_2 plane is given by a sum of the Josephson, quasiparticle, and displacement currents as

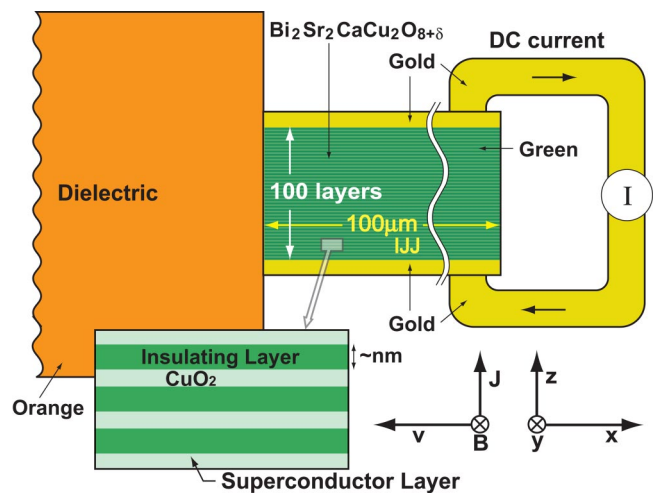


FIG. 1. (Color online) Schematic diagram of a prototype model for terahertz emission. $\text{Bi}_2\text{Sr}_2\text{CaCu}_2\text{O}_{8+\delta}$ forms the IJJ shown in green, and electrode gold plates form the top and bottom electrodes shown in yellow. A dielectric wave guide shown in orange extends from the left surface of the IJJ.

$$J_{z,l+1,l}(\mathbf{r},t) = J_c \sin \psi_{l+1,l}(\mathbf{r},t) + \sigma_c E_{z,l+1,l}(\mathbf{r},t) + \frac{\varepsilon_c}{4\pi} \partial_t E_{z,l+1,l}(\mathbf{r},t), \quad (1)$$

where J_c is the critical current in zero magnetic field, σ_c is the normal conductivity along the c axis, and $E_{z,l+1,l}$ is the electric field between $(l+1)$ th and l th layers along the z axis. The $\psi_{l+1,l}$ is the gauge invariant phase difference defined as

$$\psi_{l+1,l}(\mathbf{r},t) = \varphi_{l+1}(\mathbf{r},t) - \varphi_l(\mathbf{r},t) - \frac{2\pi}{\phi_0} \int_{z_l}^{z_{l+1}} dz A_z(\mathbf{r},z,t), \quad (2)$$

with the vector potential $A_z(\mathbf{r},z,t)$ and the flux unit ϕ_0 . For the superconducting current densities in the CuO_2 plane, we use the generalized London equations, since the Ginzburg-Landau parameter is very large in cuprate superconductors. We insert Eqs. (1) and (2) into Maxwell's equations along with the superconducting current in the ab planes and the charging effect in the CuO_2 plane. Following the calculation procedure given in Ref. 7 and after cumbersome calculations, we have

$$(1 - \zeta \Delta^{(2)}) \{ (\partial_t^2 \psi_{l+1,l} + \beta \partial_t \psi_{l+1,l} + \sin \psi_{l+1,l}) + \alpha s' [\partial_t (\rho'_{l+1} - \rho'_l) + \beta (\rho'_{l+1} - \rho'_l)] \} = \partial_x^2 \psi_{l+1,l} + \partial_y^2 \psi_{l+1,l}, \quad (3)$$

$$s' (1 - \alpha \Delta^{(2)}) \rho'_l = \partial_t (\psi_{l+1,l} - \psi_{l,l-1}). \quad (4)$$

In the above equation, we use normalized units for length, time, and charge density in the l th CuO_2 plane, respectively, defined as

$$x' = \frac{x}{\lambda_c}, \quad t' = \omega_p t, \quad \text{and} \quad \rho'_l = \frac{\lambda_c \omega_p \rho_l}{j_c}, \quad (5)$$

where ρ_l is the charge density in the l th CuO_2 layer. The plasma gap frequency is given by $\omega_p = c / (\sqrt{\varepsilon_c} \lambda_c)$, ε_c being the dielectric constant along the z axis and λ_c being the magnetic field penetration depth from the bc surface plane. The parameters in Eqs. (3) and (4) are defined as

$$\zeta = \frac{\lambda_{ab}^2}{sd}, \quad \alpha = \frac{\varepsilon_c \mu^2}{sd}, \quad s' = \frac{s}{\lambda_c}, \quad \text{and} \quad \beta = \frac{4\pi \sigma_c \lambda_c}{\sqrt{\varepsilon_c} c}, \quad (6)$$

where the s and d are the thickness of the superconducting and insulating layers, respectively. λ_{ab} is a parameter related to the current in the CuO_2 superconducting layer, and μ is the Debye screening length. The operator $\Delta^{(2)}$ is defined as $\Delta^{(2)} f_l = f_{l+1} - 2f_l + f_{l-1}$. We use Eqs. (3) and (4) in the IJJ and use Maxwell's equations in the dielectric, and outer space to simulate the emission of terahertz wave.

If Eqs. (3) and (4) are linearized, we obtain the Josephson plasma solution. The Josephson plasma is a composite wave of the Josephson current and the electromagnetic wave. The amplitudes of the Josephson current and the electric field are always parallel to the c axis. Depending on the wave propagation directions parallel to the c axis and the a axis, there appear, respectively, the longitudinal and transverse plasma waves. The transverse and longitudinal waves have been observed by Tamasaku *et al.*,⁸ and Matsuda *et al.*,⁹ respectively.

Let us show how the plasma wave is converted to the electromagnetic wave at the interface between the IJJ and the dielectric. As mentioned before, the plasma waves have transverse and longitudinal components. However, the electromagnetic wave has only the transverse component. Therefore, only the transverse plasma wave can convert into the electromagnetic wave at the interface. When we solve Eqs. (3) and (4), we impose the following boundary condition. To connect the Josephson plasma wave in the IJJ to the electromagnetic wave in the dielectric at the interface, we put the usual electromagnetic boundary condition; the electric and magnetic fields parallel to the interface are continuous at the interface. The electromagnetic wave in the dielectric is assumed to transmit freely to outer space at the end surface of the dielectric. One possible way to achieve this condition is to make a gradation of the dielectric constant near the surface. It is assumed that the opposite surface of the IJJ is exposed to vacuum.

Keeping in mind that the IJJ is $\text{Bi}_2\text{Sr}_2\text{CaCu}_2\text{O}_{8+\delta}$ and the dielectric is MgO , we chose $\lambda_{ab} = 0.4 \mu\text{m}$, $\lambda_c = 200 \mu\text{m}$, $s = 3 \text{ \AA}$, $d = 12 \text{ \AA}$, $\mu = 0.6 \text{ \AA}$, $\alpha = 0.1$, $\beta = 0.01 - 0.05$, and the number of layers = 20–1000, and take the dielectric constants along the z axis in the IJJ and the dielectric constant of MgO to be $\varepsilon = 10$. We apply a magnetic field of 1 T along the y axis. We supply an external current from the gold electrodes shown in yellow in Fig. 1. We change the normalized external current J/J_c from 0.0 to 1.5 in steps of 0.0125. The superconductivity in the top and bottom electrodes is assumed to penetrate to $0.075 \mu\text{m}$. We note that for the external currents mentioned above, the superconducting current component of J is always less than J_c . The length of the IJJ is taken to be $100 \mu\text{m}$ along the x axis and the length of the dielectric is taken to be $50 \mu\text{m}$ along the x axis. For each external current, the time evolution is simulated until the system reaches a stationary state, that is normalized time $t' = 600$, and the emission power is calculated after that time.

We assume that the system is uniform along the y axis and make two-dimensional calculation in the x - z plane. We use the finite difference method to perform the numerical simulation. The simulation uses very large sized nonlinear equations heretofore difficult to compute. Therefore, we used the Earth Simulator that has a peak performance of 40 teraflops, and is of a vector-parallel type.

Let us consider a case that the node-less Josephson plasma wave along the z axis (the transverse plasma) can be converted into the electromagnetic wave with the same frequency. In this case the emitted electromagnetic wave propagates approximately in the negative direction of the x axis. We found that the stacking number that fulfills the condition is 100 layers under the magnetic field of 1 T.

The fluxons form a triangle lattice at zero external currents. When an external current is applied, the lattice moves with a small oscillation of fluxons. When the current exceeds a critical value, clusters are formed with disordered fluxons as shown in Fig. 2, and in this dynamical phase the oscillation amplitude of fluxons and the coherent oscillation amplitude of the superconducting phase anomalously increase. This increase enhances the oscillating electromagnetic field. Figure 2 shows snapshots of the moving fluxons and the oscillating electric fields in the cases $\beta = 0.02$ and $\beta = 0.03$. In the

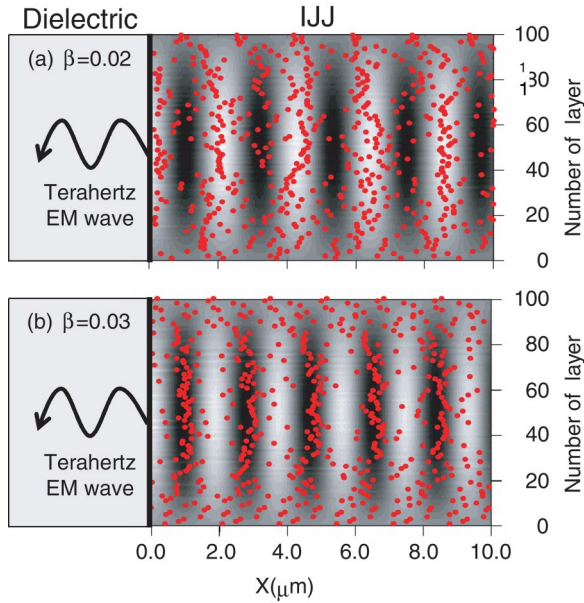


FIG. 2. (Color online) A snapshot of moving fluxons and the oscillating electric fields of the standing plasma waves in the two cases of (a) $J/J_c=0.6$, $\beta=0.02$ and (b) $J/J_c=1.0$, $\beta=0.03$.

figure the static and uniform electric field have been subtracted. The red dots show the centers of the fluxons. The fluxons move in the negative direction of the x axis direction with a large phase oscillation. The speeds of the fluxons in the applied magnetic field of 1 T are about 4% and 4.5% of the light velocity for the currents $J/J_c=0.6$, $\beta=0.02$ and $J/J_c=1.0$, $\beta=0.03$, respectively. The magnetic field of a fluxon spreads in the range of λ_c along the ab plane. For a magnetic field of 1 T 6000 fluxons are contained in the IJJ. Therefore, the magnetic field of the moving fluxons is almost uniform and thus the fluxon flow creates an almost uniform voltage between the layers. The voltage induces the oscillating current due to the Josephson effect and the oscillating current excites the Josephson plasma. The plasma wave is reflected at the interface between the IJJ and the dielectric and at the surface exposed to vacuum, and it forms an approximate standing wave in the stationary state as observed in Fig. 2.¹⁰ In Fig. 2 white parts show the electric field directing to the z axis, and dark parts show the electric field directing to negative direction of the z axis.

Figure 3 shows a snapshot of the electric and magnetic fields of the standing wave at the 50th insulating layer from the bottom surface in the direction of the z axis. The standing wave of the electric field along the z axis oscillates with 2.86 THz around a constant electric field for the normalized current $J/J_c=0.8$ and for $\beta=0.02$. The red line shows the interface between the dielectric and the IJJ. The components of the electric and magnetic fields parallel to the interface fulfill the electromagnetic continuity condition at the interface. In Fig. 3 the green curves indicate the magnetic and electric fields at the time of 1.2769 ns after the system attains to the stationary state, and the brown dotted curves indicate the magnetic and electric fields at the time of 1.2772 ns. The belly of an electric field oscillation with the largest amplitude is pinned at the interface, inducing the large amplitude of the

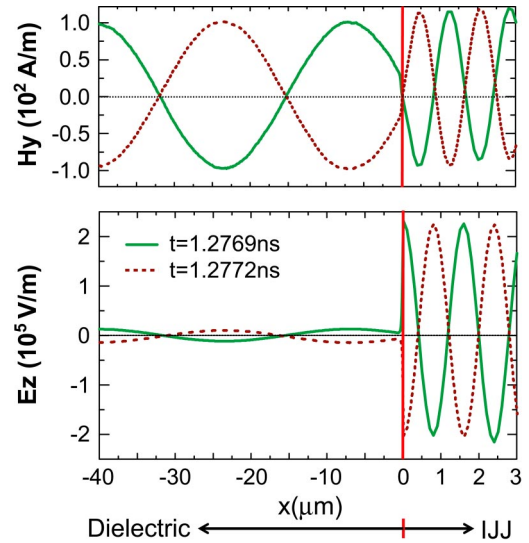


FIG. 3. (Color online) Snapshot of the plasma wave that is a standing wave in the IJJ and the electromagnetic wave that is a propagating wave in the dielectric.

electric and magnetic field oscillations in the dielectric. The ratio of the electric field to the magnetic field at $4 \mu\text{m}$ from the interface is equal to that of the usual electromagnetic wave. The present emission mechanism of the coherent terahertz electromagnetic wave is similar to a laser mechanism. The IJJ itself works as a cavity. The input energy is stored in the form of a standing Josephson plasma in the IJJ. A few percent of the energy is emitted as a terahertz electromagnetic wave from the IJJ to the dielectric through the interface.

Figure 4 shows the current-voltage characteristic curve calculated by using Eqs. (2) and (3) for $\beta=0.02$. The terahertz plasma wave occurs from $J/J_c=0.55$ to $J/J_c=1.00$ in the region where the voltage increases almost linearly as a function of the current. In this region the gauge invariant phase difference $\psi_{l+1,l}(\mathbf{r}, z, t)$ is expressed by a sum of the translationally moving part $\psi_{l+1,l}^0(\mathbf{r}, z, t)$ and the oscillating part $\Phi_{l+1,l}(\mathbf{r}, z, t)$ as $\psi_{l+1,l}(\mathbf{r}, z, t) = \psi_{l+1,l}^0(\mathbf{r}, z, t) + \Phi_{l+1,l}(\mathbf{r}, z, t)$.

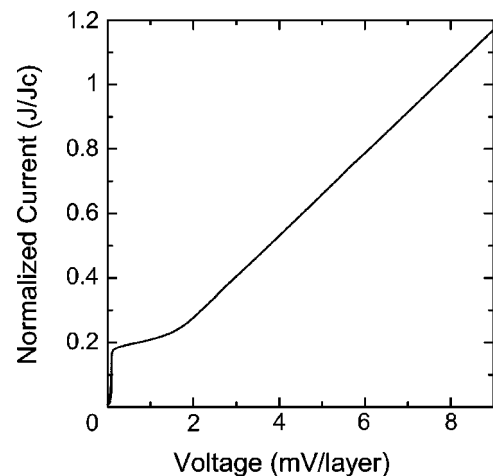


FIG. 4. Current-voltage characteristic for $\beta=0.02$.

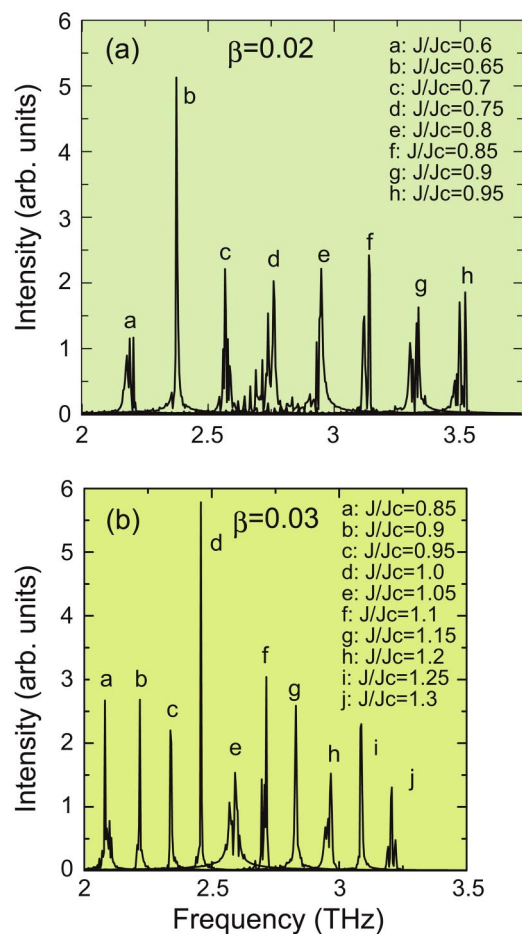


FIG. 5. (Color online) (a) and (b), respectively, show the frequency spectra calculated FFT analysis for $\beta=0.02$ and 0.03 for several normalized currents. The intensity is obtained by calculating the Poynting vector at a location of $4 \mu\text{m}$ from the interface.

The phase $\psi_{l+1,l}^0(\mathbf{r},z,t)$ mainly contributes to the current-voltage characteristic in this region and $\Phi_{l+1,l}(\mathbf{r},z,t)$ mainly contributes to formation of the plasma wave. In the other regions the coherent plasma oscillation cannot occur due to incoherence among the phases in different layers or due to formation of the moving fluxon lattice order. The peculiar feature of the current-voltage characteristic in low current region in Fig. 4 remains to be explained.

In Fig. 5 we show the frequency spectra calculated by fast Fourier transform analysis of the electromagnetic wave at a location $4 \mu\text{m}$ from the interface for the cases of $\beta=0.02$ and 0.03 . Figure 5(a) shows that when J/J_c is changed from 0.6 to 0.95 , the frequency of the emitted electromagnetic wave is changed from 2.2 to 3.5 THz, and Fig. 5(b) shows that when J/J_c is changed from 0.85 to 1.3 , the frequency is changed from 2.1 to 3.2 THz. The frequency spectrum for a fixed current shows the satellites around the sharp peak. This behavior can be explained in the following way. The sharp peak comes from the plasma excited by the ac Josephson effect. The phase difference $\Phi_{l+1,l}(\mathbf{r},z,t)$ oscillates with the frequency the same as the plasma frequency, since $E_{z,l+1,l}(\mathbf{r},t)$ is proportional to $\partial/\partial t \Phi_{l+1,l}(\mathbf{r},z,t)$. In addition to the oscillation, the interaction between the fluxon clusters

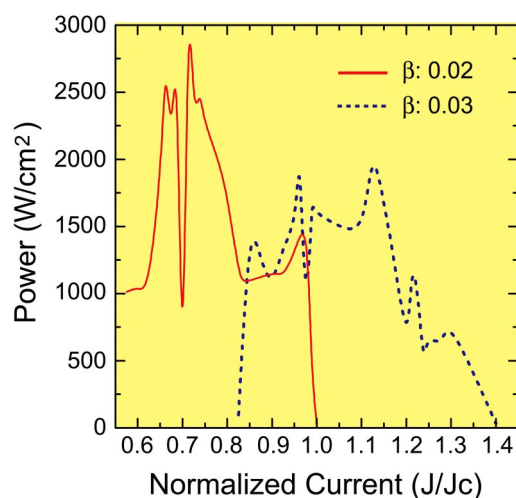


FIG. 6. (Color online) The emission power (W/cm^2) of the electromagnetic wave as a function of the external current. J_c is taken to be $800 \text{ A}/\text{cm}^2$.

causes the fluxon oscillations and thus it causes the oscillations of the phase $\Phi_{l+1,l}(\mathbf{r},z,t)$ with small frequencies compared with the plasma frequency. The fluxon oscillations interact with the plasma oscillation causes the satellites around the plasma peak. This fact may be understood from comparison of Figs. 2 and 5. The fluxon clusters along the x axis in Fig. 2(b) are narrower than those in Fig. 2(a), and thus the interaction between the fluxon clusters in former is weaker than that in the latter. This fact is consistent with the fact that the satellite intensity in Fig. 5(b) is weaker than that in Fig. 5(a). The frequency of the electromagnetic wave emitted from the IJJ varies continuously with changing current J/J_c , indicating that this emission of the sample is frequency tunable. The frequencies calculated by the simulation are equal to the ac Josephson frequency estimated by the fluxon flow voltage within the accuracy of 1.3% . This fact suggests that the plasma wave is excited by the oscillating current through the ac Josephson effect.

Figure 6 shows the emission power (the Poynting vector) measured in the dielectric at the location $4 \mu\text{m}$ from the interface as a function of the external current. The emission occurs in some limited current region as seen in Fig. 6. When the current is smaller than a critical value, the emission power propagating perpendicular to the interface vanishes. The reason is the appearance of nodes in the oscillating electric field along the z axis, indicating inclusion of the longitudinal component, and thus the emission power vanishes as mentioned before. When the current is larger than an upper critical value, the fluxons take various dynamical orders.¹¹ According to the dynamical orders, the emission is abruptly weakened, since the rigidity of the moving lattice suppresses fluxon oscillations. When β decreases, for example $\beta=0.01$, the oscillations of electric and magnetic fields lose the coherence and the emission power vanishes. When β increases, the friction for moving fluxons becomes larger and the emission power decreases.

In the present paper we performed the simulation of terahertz wave emission with the parameters corresponding to

$\text{Bi}_2\text{Sr}_2\text{CaCu}_2\text{O}_{8+\delta}$, and obtained the following results: The sample works as a cavity, and the input energy is stored in a form of standing wave of the Josephson plasma. A part of the energy is emitted as terahertz waves. The emission of electromagnetic waves is in the form of continuous coherent terahertz waves with power of 2000 W/cm^2 in the present model. The frequency can be tuned by changing the applied current. The detailed calculations and the results for general cases will be published elsewhere.

ACKNOWLEDGMENTS

The authors thank T. Sato to permit us for using the Earth Simulator and Y. Kanada for the benefit of our use of SR8000. The authors thank J. Nishizawa, K. Kadowaki, L. N. Bulaevskii, A. E. Koshelev, T. Yamashita, T. Hatano, Y. Takano, K. Hirata, H. Wang, S. Kim, T. Tachiki, T. Koyama, M. Machida, H. Matsumoto, and G. Prabhakar for valuable discussions.

¹T. Koyama and M. Tachiki, *Solid State Commun.* **96**, 367 (1995).

²A. V. Ustinov, H. Kohlstedt, and P. Henne, *Phys. Rev. Lett.* **77**, 3617 (1996).

³G. Hechtfisher, R. Kleiner, A. V. Ustinov, and P. Mueller, *Phys. Rev. Lett.* **79**, 1365 (1997).

⁴P. Barbara, A. B. Cawthorne, S. V. Shitov, and C. J. Lobb, *Phys. Rev. Lett.* **82**, 1963 (1999).

⁵M. Tachiki, T. Koyama, and S. Takahashi, *Phys. Rev. B* **50**, 7065 (1994).

⁶L. N. Bulaevskii, M. P. Maley, and M. Tachiki, *Phys. Rev. Lett.* **74**, 801 (1995).

⁷For example, see M. Tachiki, T. Koyama, and S. Takahashi, in *Coherence in High Temperature Superconductor*, edited by G. Deutscher and A. Revcolevschi (World Scientific, Singapore, 1996), p. 371.

⁸K. Tamasaku, Y. Nakamura, and S. Uchida, *Phys. Rev. Lett.* **69**, 1455 (1992).

⁹Y. Matsuda, M. B. Gaifullin, and K. Kumagai, *Phys. Rev. Lett.* **75**, 4512 (1995).

¹⁰T. Clauss, T. Uchida, M. Möhle, D. Koelle, and R. Kleiner, *Appl. Phys. Lett.* **85**, 3166 (2004).

¹¹A. E. Koshelev and I. Aranson, *Phys. Rev. B* **64**, 174508 (2001).